Microbial rhodopsins are increasingly favored over chlorophyll in High Nutrient Low Chlorophyll waters

Babak Hassanzadeh[1], Blair Thomson[2], Fenella Deans[2], Jess Wenley[2], Scott Lockwood[2], Kim Currie[2], Sergio E. Morales[2], Laura Steindler[3], Sergio A. Sañudo-Wilhelmy[1], Federico Baltar[4], Laura Gómez-Consarnau[1,5*]

[1]University of Southern California, Los Angeles, CA, United States; [2]University of Otago, Dunedin, New Zealand; [3]University of Haifa, Department of Marine Biology, Leon H. Charney School of Marine Sciences, Haifa, Israel; [4]University of Vienna, Dept. of Functional & Evolutionary Ecology, Vienna, Austria; [5]Centro de Investigación Científica y de Educación Superior de Ensenada, Ensenada, BC, Mexico.

*Correspondence: gomezcon@usc.edu

Keywords: Microbial rhodopsin, proteorhodopsin, phytoplankton, bacterioplankton, photoheterotrophy, chlorophyll, HNLC.

Running title: Microbial rhodopsins in High Nutrient Low Chlorophyll waters

Originality-Significance statement: High Nutrient Low Chlorophyll (HNLC) regimes cover approximately 30% of the global ocean surface and play a crucial role in the Earth's carbon cycle. Here we show that microbial rhodopsins are particularly abundant in a HNLC region of the Subantarctic ocean, where chlorophyll abundance is relatively low and photosynthesis and respiration might be impaired due to iron limitation. These data suggest that rhodopsin phototrophy can contribute significantly to the energy budgets of HNLC regions, capturing meaningful amounts of light that cannot be channeled through photosynthesis.

Abstract

Microbial rhodopsins are simple light-harvesting complexes that, unlike chlorophyll photosystems, have no iron requirements for their synthesis and phototrophic functions. Here we report ~~the first~~ environmental concentrations of rhodopsin along the Subtropical Frontal Zone off New Zealand, where Subtropical waters encounter the iron-limited Subantarctic High Nutrient Low Chlorophyll (HNLC) region. Rhodopsin concentrations were highest in HNLC waters where chlorophyll-*a* concentrations were lowest. Furthermore, while the ratio of rhodopsin to chlorophyll-*a* photosystems was on average 20 along the transect, this ratio increased to over 60 in HNLC waters. We further show that microbial rhodopsins are abundant in both picoplankton (0.2-3μm) and in the larger (>3μm) size fractions of the microbial community containing eukaryotic plankton and/or particle-attached prokaryotes. These findings suggest that rhodopsin phototrophy could be critical for microbial plankton to adapt to resource-limiting environments where photosynthesis and possibly cellular respiration are impaired.

Introduction

The Subantarctic region of the Southern Ocean is a crucial regulator of the global climate system. Not only is it one of the largest sinks of atmospheric CO_2 in the world ocean (Metzl *et al*., 1999), but also the source of nutrients that ultimately fuel most of the global ocean's primary production through the convective formation of intermediate waters in this region (Toggweiler *et al*., 1991; Sarmiento *et al*., 2004). For that reason, the importance of chlorophyll-based photosynthesis in the Subantarctic waters to the global carbon budget has been studied for decades (Boyd *et al*., 1999; Doblin *et al*., 2011). Yet, the magnitude of rhodopsin-based phototrophy and its role in sustaining microbial communities in the Subantarctic HNLC oceanographic regime remains unknown. Microbial rhodopsins are light-driven ion-pumps (Béjà *et al*., 2000) present in microorganisms of all life domains, with notably over 80% of the surface marine bacteria containing these genes (Dubinsky *et al*., 2017; Sieradzki *et al*., 2018). The simplicity and low synthesis cost of rhodopsin photosystems compared to chlorophyll further suggest that they have a critical role in light energy acquisition, particularly in resource deplete environments where photosynthesis is limited (Raven, 2009). Supporting this hypothesis, several culture studies have shown that rhodopsin phototrophy can improve bacterial growth, survival, or reduce respiration rates when labile organic matter resources are scarce (Gómez-Consarnau *et al.,* 2007; 2010; Steindler *et al.,* 2011). Also, *in situ*, the abundance of rhodopsin genes appears to be negatively correlated to chlorophyll and inorganic nutrient concentrations (Campbell *et al*., 2008). To date, ambient rhodopsin concentrations (i.e., the number of rhodopsin photosystems per volume of seawater) have only been reported for the Mediterranean Sea and the Eastern Atlantic Ocean, where they also tended to be inversely related to phytoplankton biomass, nitrate, and phosphate concentrations (Gómez-Consarnau *et al*., 2019). Despite this empirical evidence, not all studies on rhodopsin phototrophy reflect a clear association with macronutrients or

organic matter availability, suggesting that other regulating factors may exist (Pinhassi *et al*., 2016). For instance, a study in the Chesapeake Bay found that the percent of rhodopsin-containing cells was positively correlated to salinity using a microscopy-based method (Keffer *et al*., 2015; Maresca *et al*., 2018). Therefore, expanding rhodopsin observations to additional key marine regions is essential to further elucidate their regulation mechanisms and overall importance globally.

The relationship between rhodopsin phototrophy and iron availability has not been tested thoroughly, and never in the HNLC Subantarctic waters where microbial growth is limited by the availability of this trace element (Sedwick *et al*., 1999; Sander *et al*., 2015). Unlike chlorophyll-based photosynthesis, rhodopsin phototrophy does not involve any known redox reactions, and its functioning is independent of electron carriers such as iron (Raven, 2009). Rhodopsin-like genes have been found in populations of the diatom *Pseudo-nitzschia granii* from the North Pacific HNLC region, and further culture studies revealed that the highest levels of both rhodopsin transcripts and proteins occur under low iron conditions in a *P. granii* strain (Marchetti *et al*., 2015). This suggests that this diatom may, indeed, rely on rhodopsin phototrophy when iron concentrations are insufficient to adequately perform photosynthesis. Furthermore, given the high iron requirements of the respiratory electron transport chain, heterotrophic bacterial respiration can also be impaired in HNLC regions due to iron limitation (Tortell *et al*., 1996).

Results and Discussion

Here we studied the distributions of the two most important solar energy transducing systems, rhodopsin and chlorophyll-*a* (chl-*a*), on a 60 km transect across the Subtropical Frontal Zone off New Zealand (Munida Microbial Observatory Time Series; MOTS), which traverses through three contrasting oceanographic regimes and water masses: Coastal neritic (CNW), Subtropical (STW), and Subantarctic waters (SAW) (Jillett, 1969) (Figure 1A and Supplementary Information). This geographical transect provides a unique opportunity to evaluate the relative contribution of each photosystem in three contrasting environments ranging from coastally-influenced waters to an HNLC iron-limited region (Figure 1B).

Surface rhodopsin and chl-*a* concentrations displayed particular spatial and temporal trends along the transect; rhodopsin ranged from 7 to 27 pM (Figure 1C) while chlorophyll varied substantially more (16-fold; 100-1600 pM; Figure 1D). The highest chl-*a* concentrations were found in different size fractions, depending on the sampling station and season. Rhodopsins were present in all size fractions of the microbial community, with more than 35% of the signal being found in the large size fractions (>3µm). Although rhodopsin genes and transcripts had previously been identified in large microbial communities (>0.8µm) in a temperate estuary (Maresca *et al*., 2018), these are the first data reporting actual rhodopsin quantifications in nano- or micro-plankton in any open-waters marine system, indicating their presence in eukaryotes and/or particle-attached prokaryotes. However, most of the total rhodopsin content (62%) was found in the picoplankton fractions. These observations, together with rhodopsin gene data from the global ocean (Pinhassi *et al*., 2016), suggest that rhodopsin phototrophy is widespread in marine microbial communities and that it is primarily a prokaryotic light-capturing feature.

Rhodopsins reached their highest concentrations (~30 pM) at the SAW HNLC stations, coinciding with the lowest chl-*a* levels (100-140 pM; Figures 1CD, 2A), suggesting an increased prevalence of rhodopsin-containing microbial plankton or cellular rhodopsin quotas in the HNLC region. The vertical distributions of rhodopsin (Figure 2A) revealed a maximum above the deep chlorophyll maximum, with less vertical fluctuations than chl-*a*. Within a given depth profile, chl-*a* concentrations fluctuated between 2-4-fold, while rhodopsin levels varied <2-fold. The depth distributions of these photosystems are consistent with previous observations (Gómez-Consarnau *et al*., 2019) and with the notion that rhodopsin synthesis is energetically advantageous only at high irradiances (Kirchman and Hanson, 2013).

Rhodopsin photosystem abundances were on average 20 times higher than those of chl-*a* throughout the transect. Yet in HNLC waters, the ratio of rhodopsin to chl-*a* photosystems (R:C ratio) was significantly higher than in the other regions (40±11 compared to 10±5; Figure 2B), suggesting an increase in photoheterotrophy over photosynthesis associated with water mass characteristics (Figure 1B). Similarly, Marchetti et al. (2015) reported an increase in the relative abundance of rhodopsin transcripts and proteins for the diatom *P. granii* under iron deplete conditions. Our observations in natural microbial communities of this HNLC region suggest that the increased R:C photosystem ratios could also be caused by physiological changes within the cells, as observed in *P. granii*. However, we cannot rule out an increase due to the presence of a larger number of rhodopsin-utilizing organisms.

Picoplankton displayed the highest R:C ratios, increasing 3-fold from 21±5 in the STW and CNW to 68±21 in the SAW-HNLC region (Figure 2B). Thus, while there are several known microbial strategies for coping with iron stress (e.g., the production of siderophores (Tagliabue *et*

135 *al*., 2017); high affinity transporters and decreased cell size (Sunda and Hunstman, 1997)), our
136 data show that HNLC environments appear to be selectively enriched with microbial
137 communities that can cope with iron stress by harvesting sunlight through rhodopsins when
138 photosynthesis and/or respiration are compromised. In fact, the metabolic versatility gained
139 through rhodopsin photoheterotrophy may explain the relatively similar bacterial abundances and
140 respiration rates previously reported in STW and SAW despite substantial differences in iron
141 availability (Baltar *et al*., 2015). Given that respiration is the most iron-demanding process and
142 the primary energy-generating mechanism in heterotrophs (Raven, 1988), the increase in R:C
143 among picoplankton suggests that rhodopsin energy capture provides an ecological advantage
144 during iron limitation. Furthermore, it implies that there is an additional and still unknown
145 amount of solar energy fueling HNLC ecosystems that needs to be considered in energy budgets.
146 Identifying the major rhodopsin-containing microbial groups (both heterotrophs and eukaryotic
147 phytoplankton) in HNLC regions will be central to elucidate the potential ecological processes
148 impacted by this metabolism. Finally, revealing the intricacies of rhodopsin phototrophy as a
149 coping mechanism against resource limitation is likely to reshape our understanding of energy
150 acquisition and the present and future carbon cycle in the ocean.

151

152 **Materials and Methods**

153 Seawater samples were collected from 8 stations along the MOTS transect at several
154 depths on March 26 and September 20, 2018 (Figure 1; Supplementary Information). Surface
155 seawater (2m depth) was sampled at all stations, whereas the deep chlorophyll maximum (DCM)
156 was only sampled at stations 3 and 8. Approximately 10-liter samples were size-fractionated by
157 an in-line serial filtration system (10 μm, 3μm, and 0.22 μm pore sizes) using a peristaltic pump.

Rhodopsin and chlorophyll-based photosystem concentrations were determined using retinal and chlorophyll-*a* as proxies. Both pigments were extracted from the filters with methanol (Garrido and Roy, 2015; Gómez-Consarnau *et al*., 2019). Aliquots from each extract were used for immediate fluorometric chlorophyll-*a* quantification using the non-acidification method (Knap *et al*., 1994) while retinal concentrations were determined through LC/MS/MS (Gómez-Consarnau *et al*., 2019). Rhodopsin photosystem abundances were then estimated assuming that each rhodopsin photosystem contains one molecule of retinal (Larkum *et al*., 2018) and that each chlorophyll-based photosystem contains on average 300 molecules of chl-*a* (Mirkovic *et al*., 2016). Total rhodopsin and chl-*a* concentrations were calculated by adding the three size fractions. The specific LC/MS/MS operational conditions were slightly modified from Gómez-Consarnau et al. (2019) according to Kane and Napoli (2010) to include the use of an internal standard (see Supplementary Information).

Total dissolved iron (dFe) concentrations (operationally defined as the fraction that passed through a 0.45 μm filter) used in this study were obtained from previous March and September cruises and are reported in Sander et al. (2015). The samples for dFe were stored at a pH <2 and quantified after a dithiocarbamate organic extraction (Bruland *et al*., 1979).

Figure captions

Figure 1. (A). Location of the sampling stations (shown in red) along the Munida Microbial Observatory Time Series (MOTS) in Coastal Neritic (CNW), Subtropical (STW); and Subantarctic (SAW) waters. The position of the Subtropical front, which moves seasonally, belongs to March of 2018. Temperature and salinity plots are shown in Figure S1. **(B)** Surface

concentrations of dissolved nitrate, phosphate, and iron (dFe) from discrete sampling locations. Nitrate and phosphate concentrations belong to the March and September 2018 cruises. Average dissolved iron concentrations are from previously reported cruises of March and September of years 2000-2003 (Sander *et al*., 2015). **(C)** Rhodopsin and **(D)** chlorophyll-*a* levels in picoplankton (0.2-3.0 μm), nanoplankton (3.0-10.0 μm), and >10.0 μm size fractions of the microbial community. The narrower columns in panels C-D represent photosystem concentrations from samples collected at three different depths, 2m, 20m, and deep chlorophyll maximum (from left to right).

Figure 2. (A) Depth profiles of rhodopsin and chlorophyll-*a* concentrations measured in March and September of 2018. Station-3 and station-8 were located in Subtropical (STW) and Subantarctic (SAW) waters, respectively. **(B)** Rhodopsin to chlorophyll-*a* photosystem ratios in different size fractions of the microbial community, grouped by water mass. Photosystem abundance was calculated assuming one molecule of the retinal for rhodopsin and 300 molecules of chlorophyll-*a* for each chl-*a* photosystem (Mirkovic *et al*., 2016). Rhodopsin:Chlorophyll-*a* ratios were significantly higher in the HNLC Subantarctic compared to Coastal neritic and Subtropical water masses (Welch two sample t-test, $p=6.9\cdot10^{-4}$ for 0.2-3 μm, $p=1.1\cdot10^{-3}$ for 3-10 μm, $p=6.0\cdot10^{-5}$ for >10 μm size fractions, and $p=3.3\cdot10^{-5}$ for the entire community).

Acknowledgments: We would like to thank the captain and crew of R/V Polaris II, and Hannah Adams for her assistance with pigment extractions. This research was supported by Grant No OCE1924464 from the United States National Science Foundation (NSF) to L.G.-C. and by Grant No 2019612 from the United States-Israel Binational Science Foundation (BSF) to L.S., as well as the Rutherford Discovery Fellowship to F.B.

Author Contributions: B.H., F.B., and L.G-C. designed research; B.H., B.T., F.D., J.W., S.L., K.C., S.E.M., L.S., S.A.S-W, F.B. and L.G.-C. performed research and analyzed data. B.H. and L.G.-C. wrote the manuscript with the input of all authors.

Competing Interest Statement: The authors declare no competing interest.

References

Baltar, F., Stuck, E., Morales, S., and Currie, K. (2015) Bacterioplankton carbon cycling along the subtropical frontal zone off New Zealand. *Prog Oceanogr* 135: 168-175.

Boyd, P., LaRoche, J., Gall, M., Frew, R., and McKay, R.M.L. (1999) Role of iron, light, and silicate in controlling algal biomass in subantarctic waters SE of New Zealand. *J Geophys Res Oceans* 104: 13395-13408.

Béja, O., Aravind, L., Koonin, E.V., Suzuki, M.T., Hadd, A., Nguyen, L.P. et al. (2000) Bacterial rhodopsin: evidence for a new type of phototrophy in the sea. *Science* 289: 1902-1906.

Bruland, K.W., Franks, R.P., Knauer, G.A., and Martin, J.H. (1979) Sampling and analytical methods for the determination of copper, cadmium, zinc, and nickel at the nanogram per liter level in sea water. *Anal Chim Acta* 105: 233-245.

Campbell, B.J., Waidner, L.A., Cottrell, M.T., and Kirchman, D.L. (2008) Abundant proteorhodopsin genes in the North Atlantic Ocean. *Environ Microbiol* 10: 99-109.

Doblin, M.A., Petrou, K.L., Shelly, K., Westwood, K., Van den Enden, R., Wright, S. et al. (2011) Diel variation of chlorophyll-a fluorescence, phytoplankton pigments and productivity in the Sub-Antarctic and Polar Front Zones south of Tasmania, Australia. *Deep Sea Res Part II: Top Stud Oceanogr* 58: 2189-2199.

Dubinsky, V., Haber, M., Burgsdorf, I., Saurav, K., Lehahn, Y., Malik, A. et al. (2017) Metagenomic analysis reveals unusually high incidence of proteorhodopsin genes in the ultraoligotrophic Eastern M editerranean Sea. *Environ Microbiol* 19: 1077-1090.

Garrido, J.L., and Roy, S. (2015) Natural Products From Marine Algae: Methods and Protocols. Totowa, USA: Humana Press.

Gómez-Consarnau, L., Akram, N., Lindell, K., Pedersen, A., Neutze, R., Milton, D.L., et al. (2010) Proteorhodopsin phototrophy promotes survival of marine bacteria during starvation. *PLoS Biol* 8: e1000358.

Gómez-Consarnau, L., Gonzalez, J.M., Coll-Llado, M., Gourdon, P., Pascher, T., Neutze, R., et al. (2007) Light stimulates growth of proteorhodopsin-containing marine flavobacteria. *Nature* 445: 903–910.

Gómez-Consarnau, L., Raven, J.A., Levine, N.M., Cutter, L.S., Wang, D., Seegers, B. et al. (2019) Microbial rhodopsins are major contributors to the solar energy captured in the sea. *Sci Adv* 5: eaaw8855.

Jillett, J. (1969) Seasonal hydrology of waters off the Otago Peninsula, south- eastern New Zealand. *NZ J Mar Freshwater Res* 3: 349-375.

Kane, M.A., and Napoli, J.L. (2010) Quantification of endogenous retinoids. *Methods Mol Biol* 652: 1-54.

Keffer, J.L., Sabanayagam, C.R., Lee, M.E., DeLong, E.F., Hahn, M.W., and Maresca, J.A. (2015) Using total internal reflection fluorescence microscopy to visualize rhodpsin-containing cells. *Appl Environ Micorbiol* 81:3442-3450.

Kirchman, D.L., and Hanson, T.E. (2013) Bioenergetics of photoheterotrophic bacteria in the oceans. *Environ Microbiol* Rep 5: 188-199.

Knap, A., Michaels, A., Close, A., Ducklow, H., and Dickson, A. (1994) Protocols for the Joint Global Ocean Flux Study (JGOFS) core measurements. Paris, France: UNESCO.

Larkum, A.W.D., Ritchie, R.J., and Raven., J.A. (2018) Living off the sun: chlorophylls, bacteriochlorophylls and rhodopsins. *Photosynthetica* 56: 11-43.

Marchetti, A., Catlett, D., Hopkinson, B.M., Ellis, K., and Cassar, N. (2015) Marine diatom proteorhodopsins and their potential role in coping with low iron availability. *ISME J* 9: 2745-2748.

Maresca, J.A., Miller, K.J., Keffer, J.L., Sabanayagam, C.R., and Campbell, B.J. (2018) Distribution and diversity of rhodopsin-producing microbes in the Chesapeake Bay. *Appl Environ Microbiol* 84:00137-00118.

Metzl, N., Tilbrook, B., and Poisson, A. (1999) The annual fCO_2 cycle and the air'sea CO_2 flux in the sub-Antarctic Ocean. *Tellus B Chem Phys Meteorol* 51: 849-861.

Mirkovic, T., Ostroumov, E.E., Anna, J.M., van Grondelle, R., and Scholes, G.D. (2016) Light absorption and energy transfer in the antenna complexes of photosynthetic organisms. *Chem Rev* 117: 249-293.

Pinhassi, J., DeLong, E.F., Beja, O., Gonzalez, J.M., and Pedros-Alio, C. (2016) Marine Bacterial and Archaeal Ion-Pumping Rhodopsins: Genetic Diversity, Physiology, and Ecology. *Microbiol Mol Biol Rev* 80: 929-954.

Raven, J.A. (1998) The iron and molybdenum use efficiencies of plant growth with different energy, carbon and nitrogen sources. New Phytol 109: 279-287.

Raven, J.A. (2009) Functional evolution of photochemical energy transformations in oxygen-producing organisms. *Funct Plant Biol* 36: 505-515.

Sander, S.G., Tian, F., Ibisanmi, E.B., Currie, K.I., Hunter, K.A., and Frew, R.D. (2015) Spatial and seasonal variations of iron speciation in surface waters of the Subantarctic front and the Otago Continental Shelf. *Mar Chem* 173: 114-124.

Sarmiento, J.L., Gruber, N., Brzezinski, M., and Dunne, J. (2004) High-latitude controls of thermocline nutrients and low latitude biological productivity. *Nature* 427: 56-60.

Sedwick, P.N., DiTullio, G.R., Hutchins, D.A., Boyd, P.W., Griffiths, F.B., Crossley, A.C. et al. (1999) Limitation of algal growth by iron deficiency in the Australian Subantarctic region. *Geophys Res Lett* 26: 2865-2868.

Sieradzki, E.T., Fuhrman, J.A., Rivero-Calle, S., and Gómez-Consarnau, L. (2018) Proteorhodopsins dominate the expression of phototrophic mechanisms in seasonal and dynamic marine picoplankton communities. *PeerJ* 6: e5798.

Steindler, L., Schwalbach, M.S., Smith, D.P., Chan, F., and Giovannoni, S.J. (2011) Energy starved *Candidatus* Pelagibacter ubique substitutes light-mediated ATP production for endogenous carbon respiration. *PLoS One* 6: e19725.

Sunda, W.G., and Huntsman, S.A. (1997) Interrelated influence of iron, light and cell size on marine phytoplankton growth. *Nature* 390: 389-392.

Tagliabue, A., Bowie, A.R., Boyd, P.W., Buck, K.N., Johnson, K.S., and Saito, M.A. (2017) The integral role of iron in ocean biogeochemistry. *Nature* 543: 51-59.

Toggweiler, J., Dixon, K., and Broecker, W. (1991) The Peru upwelling and the ventilation of the South Pacific thermocline. *J Geophys Res Oceans* 96: 20467-20497.

Tortell, P.D., Maldonado, M.T., and Price, N.M. (1996) The role of heterotrophic bacteria in iron-limited ocean ecosystems. *Nature* 383: 330-332.

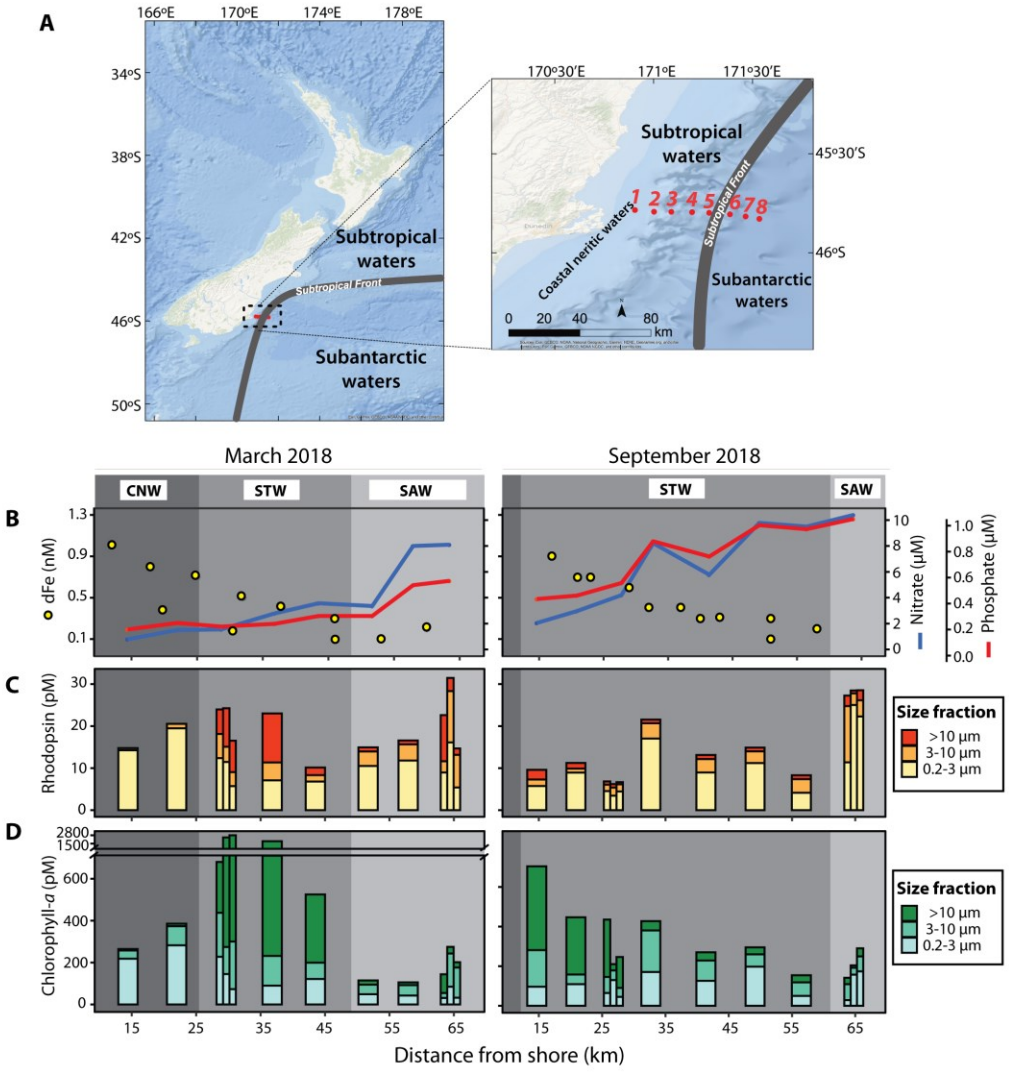
A
166°E
170°E
174°E
178°E
34°S
38°S
42°S
46°S
50°S
Subtropical waters
Subtropical Front
Subantarctic waters
170°30'E
171°E
171°30'E
45°30'S
46°S
1 2 3 4 5 6 7 8
Coastal neritic waters
0 20 40 80
km
March 2018
September 2018
CNW
STW
SAW
B
dFe (nM)
Nitrate (μM)
Phosphate (μM)
C
Rhodopsin (pM)
Size fraction
>10 μm
3-10 μm
0.2-3 μm
D
Chlorophyll-a (pM)
Distance from shore (km)

Figure 1

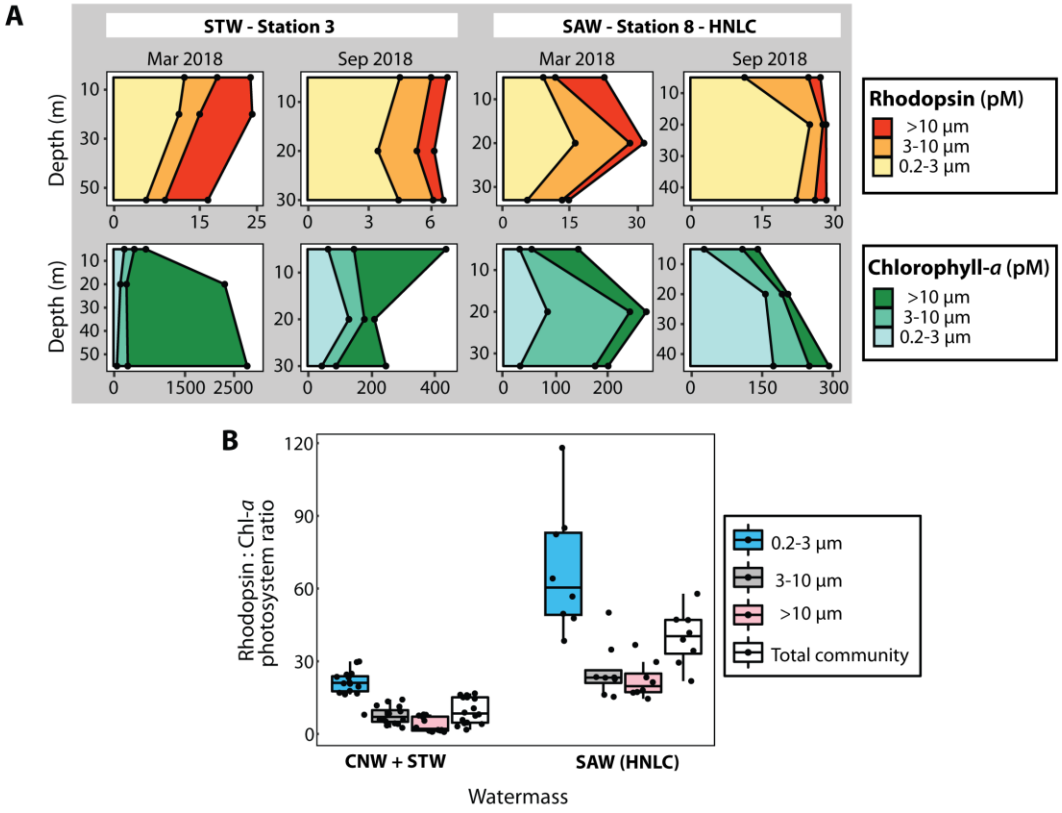
A
STW - Station 3
SAW - Station 8 - HNLC
Mar 2018
Sep 2018
Depth (m)
Rhodopsin (pM)
>10 µm
3-10 µm
0.2-3 µm
Chlorophyll-a (pM)
B
Rhodopsin : Chl-a photosystem ratio
CNW + STW
SAW (HNLC)
Watermass
Total community

Figure 2